Flexure Hinge-Based Parallel Manipulators Enabling High-Precision Micro Manipulations

I. Ivanov and B. Corves

Abstract Parallel manipulators are very suitable for the realization of planar and spatial high-precision micro manipulations, especially with flexure hinges bringing many advantages. The goal is to investigate the possibility of flexure hinges being implemented into parallel manipulators. The characteristics of typical flexure hinges are compared at first. Orthogonal parallel manipulators with a regular spatial translation of the moving platform are assessed afterwards. For a dimensioned flexure hinge and a selected parallel manipulator, a flexure hinge-based parallel manipulator is monolithically designed and analysed.

Keywords Flexure hinges · Parallel manipulators · Flexure hinge-based parallel manipulators

1 Introduction

A serial manipulator has one kinematic chain with a fixed base and a moving platform at the ends. Between them, links are serially connected by actuated joints and therefore heavily loaded. For this reason, a low positioning accuracy and a poor load capacity are available. A significant stiffness enhancement without strengthening individual links can be attained by using parallel kinematic structures. In a parallel manipulator, a moving platform is coupled with a fixed base by several separate kinematic chains, so-called limbs. Because of load distribution on the limbs, a good load capacity and a high positioning accuracy are achieved. The dynamic behaviour is also improved [1]. Parallel manipulators are very suitable for the realization of planar and spatial high-precision micro manipulations. High-precision requirements are met best with parallel kinematic structures, whose limited working spaces are not drawbacks for micro manipulations. A micro manipulation typically covers a working space up to millimetre range and a positioning accuracy up to nanometre range. Such a small working space and such a high positioning

I. Ivanov (✉)
Department of Mechanism Theory and Dynamics of Machines (IGM), RWTH Aachen University, Aachen, Germany
e-mail: ivanov@igm.rwth-aachen.de

G.K. Ananthasuresh et al. (eds.), *Micromechanics and Microactuators*, Mechanisms and Machine Science 2, DOI 10.1007/978-94-007-2721-2_6,

accuracy do not demand an extreme miniaturization, so that a micro manipulator is distinguished from a micro machine [2]. However, the micro manipulator can be implemented hardly with conventional joints, but successfully with flexure hinges. They make a monolithic design possible, which is characterized primarily by a radical reduction of backlash and friction [3]. Some applications of flexure hinge-based parallel manipulators should be mentioned: sample positioning in microscopy, wafer lithography, manufacture and assembly in precision engineering and micro system technology, etc.

2 Requirements

The selection of degrees of freedom of the moving platform depends on the function of a micro manipulator. All six degrees of freedom ensure a full mobility, but that entails high costs and a complex control. Three or four degrees of freedom are usually sufficient for a micro manipulation, namely three translations, if necessary enhanced with one rotation. The remaining degrees of freedom have to be kinematically constrained.

In precision engineering, the working space of the moving platform is normally a couple of cubic millimetres large. Since the installation space for a micro manipulator is often quite restricted, a relatively wide motion range of the flexure hinges is necessary. The motion accuracy of the flexure hinges has to be as high as possible at the same time.

Because of a monolithic design (practically no backlash in flexure hinges), environmental disturbances mainly affect the repeatability of the moving platform. Therefore, the mechanical stability (a high stiffness) and the thermal stability (a low thermal expansion) of a micro manipulator are of vital importance. Concerning calibration costs, the positioning accuracy of the moving platform should also not be neglected.

The performance test of flexure hinges or an entire micro manipulator in scanning electron microscopy is possible if applied materials are non-magnetic. For example, only austenite in case of steel, whose strength limits (yield strength and endurance strength) are rather low, is acceptable. A high ratio between the strength limits and the modulus of elasticity is preferable. However, using thermoplastics is not reasonable, because of a low modulus of elasticity. These conditions can be fulfilled with some light metal alloys (Table 1).

Table 1 Physical properties of Ti-6Al-4 V used in further research

Physical property	Symbol	Value
Mass density	ρ	4430 kg/m^3
Modulus of elasticity	E	114 GPa
Shear modulus	G	44 GPa
Yield strength	$\sigma_{0,2}$	885 MPa
Endurance strength	σ_D	515 MPa

In this paper, the characteristics (motion range and accuracy, stiffness) of typical (corner filleted notch and right circular notch) flexure hinges are compared at first. A few orthogonal parallel manipulators (3 $\underline{\mathrm{P}}\mathrm{RRRR}$, 3 $\underline{\mathrm{P}}\mathrm{RRR}$ and 3 $\underline{\Pi}\mathrm{R}\Pi\mathrm{R}$) with a regular spatial translation of the moving platform are assessed afterwards. For a dimensioned (right circular notch) flexure hinge and a selected parallel manipulator (3 $\underline{\Pi}\mathrm{R}\Pi\mathrm{R}$), a flexure hinge-based parallel manipulator is monolithically designed by means of pseudo-rigid-body modelling and analysed by means of finite-element method. Accordingly, the parasitic rotations of the moving platform, the maximum stress in the flexure hinges and the stiffness of the micro manipulator are determined.

3 Flexure Hinges

Design – If possible, revolute joints are usually combined into a universal or spherical joint for the purpose of shortening kinematic chains in case of spatial motions. A universal or spherical compliant joint (Fig. 1a-b) can be monolithically designed, but it possesses a low stiffness in all directions. A prismatic compliant joint (Fig. 1c) can be monolithically designed only as the combination of revolute compliant joints [4].

Therefore, the implementation of revolute compliant joints into parallel manipulators may be an optimal solution. Among a large number of designs, a corner filleted notch flexure hinge (Fig. 2a) and a right circular notch flexure hinge (Fig. 2b) are considered before the other ones. The characteristics of an elliptical notch flexure hinge (Fig. 2c) and similar designs stand between those of the corner filleted notch flexure hinge and the right circular notch flexure hinge [5].

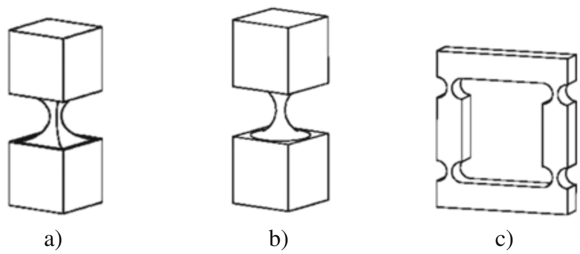

Fig. 1 Examples of universal (**a**), spherical (**b**) and prismatic (**c**) compliant joint

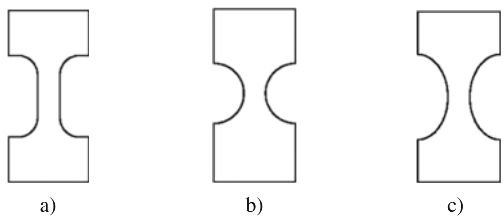

Fig. 2 Corner filleted notch (**a**), right circular notch (**b**) and elliptical notch (**c**) flexure hinge

Motion range and accuracy – In order to maximize the efficiency with regard to the motion range, a flexure hinge can be dimensioned for the maximum rotation angle (δ_{max}) corresponding to the maximum stress (σ_{max}) near to the strength limit ($\sigma_{0,2}$ or σ_D) [6]

$$\sigma_{\max} = \frac{6 \cdot K \cdot \delta_{\max}}{b \cdot t^2} \leq \sigma_D \tag{1}$$

where K is the stiffness of the flexure hinge around the rotation axis, namely

$$K_{CF} = \frac{E \cdot t^3 \cdot b}{12 \cdot l} \quad \text{for corner filleted notch} \tag{2}$$

$$K_{RC} = \frac{2 \cdot E \cdot t^{2.5} \cdot b}{9 \cdot \pi \cdot R^{0.5}} \quad \text{for right circular notch} \tag{3}$$

flexure hinges according to [7]. The design parameters of corner filleted notch and right circular notch flexure hinges are shown in Fig. 3. The design parameter b is the width of flexure hinges.

If the working space of the moving platform of 4 x 4 x 4 mm^3, which approximately needs the maximum rotation angle of the flexure hinges of ± 0.02 rad with the length of the links of 100 mm, is intended, the following design parameters can be obtained using equations (1)-(3) (Table 2):

Generally, for similar lengths, a corner filleted notch flexure hinge shows a slight stress concentration and a big rotation axis drift, while a right circular notch flexure hinge has a stabile rotation axis and an intensive stress concentration (Fig. 4) (Table 3).

Stiffness - In contrast to a conventional joint, theoretically with no stiffness in moving directions and an infinitely high stiffness in constrained directions, a flexure hinge possesses a finite stiffness in all directions. Accordingly, it is necessary to achieve adequate stiffness ratios between moving and constrained directions by the design of flexure hinges.

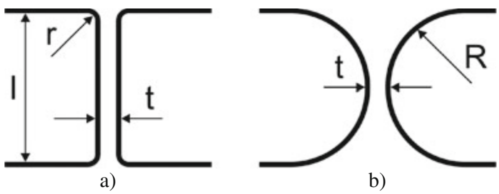

Fig. 3 Design parameters of corner filleted notch (**a**) and right circular notch (**b**) flexure hinges

Table 2 Design parameters of flexure hinges used in further research (see Fig. 3)

Corner filleted notch (r = 0.2 mm)	l = 2 mm	t = 0.4 mm	b = 20 mm
Right circular notch	R = 2 mm	t = 0.4 mm	b = 20 mm

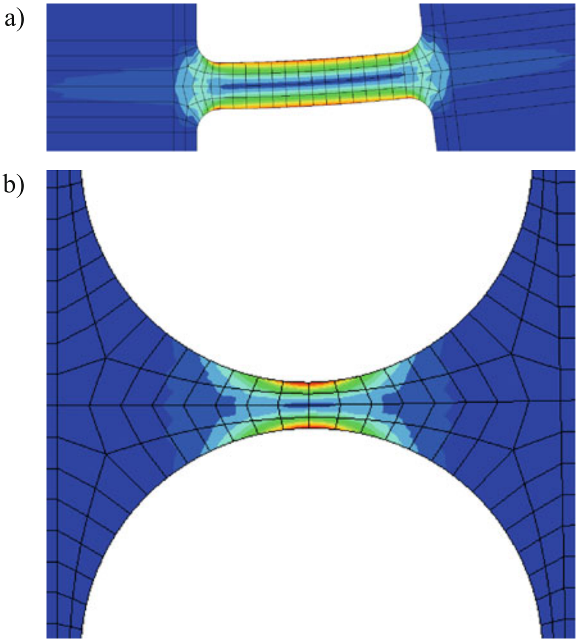

Fig. 4 Stress distribution in corner filleted notch (**a**) and right circular notch (**b**) flexure hinge (FEM)

Table 3 Maximum stress and rotation axis drift of flexure hinges for rotation angle of ±0.02 rad (FEM)

Flexure hinge	Max. stress	Axis drift
Corner filleted notch	263.1 MPa	5.067 μm
Right circular notch	419.2 MPa	3.699 μm

Table 4 Stiffness values of flexure hinges

Load type	Corner filleted notch	Right circular notch
Bending around rotation axis	6.08 Nm/rad	11.54 Nm/rad
Bending around constrained axis	15.20 kNm/rad	17.06 kNm/rad

Using the stiffness matrix according to [7], it can be calculated that the right circular notch flexure hinge is bending stiffer around the rotation axis than the corner filleted notch flexure hinge (Table 4). That as well as a higher torsion stiffness are proven by means of finite-element method (FEM) (Table 5).

Because of more suitable characteristics (motion accuracy, torsion stiffness), the right circular flexure hinge is implemented into a selected parallel manipulator here.

Table 5 Eigenfrequencies of flexure hinges (FEM)

Eigenmodes	Corner filleted notch	Right circular notch
Bending around rotation axis	10.27 Hz	13.93 Hz
Bending around constrained axis	372.5 Hz	381.8 Hz
Torsion around constrained axis	367.1 Hz	538.8 Hz

4 Parallel Manipulators

In order to compensate the effects of thermal expansion, a micro manipulator should have a symmetric fully parallel kinematic structure. Accordingly, all the limbs possess identical kinematic chains standing in a uniform circular arrangement and orientation. Moreover, an orthogonal arrangement and orientation of the limbs (Fig. 5) is preferable in case of a regular spatial translation of the moving platform [6]. Besides, all the limbs are driven in the same way. Among existing drive concepts, one with all the actuators on the fixed base shows optimal characteristics [8].

Various approaches have been used for the structure synthesis of parallel manipulators with fewer than six degrees of freedom. They have usually been based either on the group theory [9] or on the screw theory [10]. A combined approach including the group theory and the screw theory with the specifics of micro manipulation is applied here. The results are also compared with those of other approaches [11].

Three limb structures being able to build orthogonal parallel manipulators with a regular spatial translation of the moving platform are preselected and briefly assessed below.

P̲UU or P̲RRRR limb (Fig. 6) has five degrees of freedom and comprises two parallel universal joints (U) or two pairs of parallel revolute joints (R) as well as one

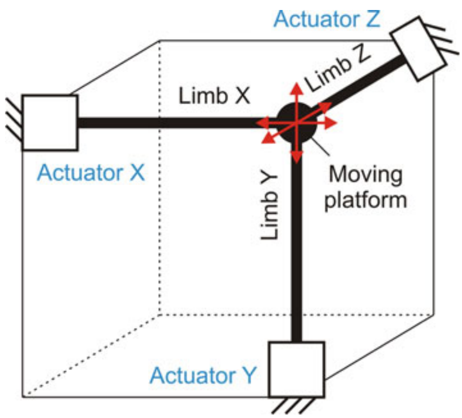

Fig. 5 Orthogonal arrangement and orientation of limbs in parallel manipulator

Fig. 6 $\underline{P}_xR_zR_yR_yR_z$ limb

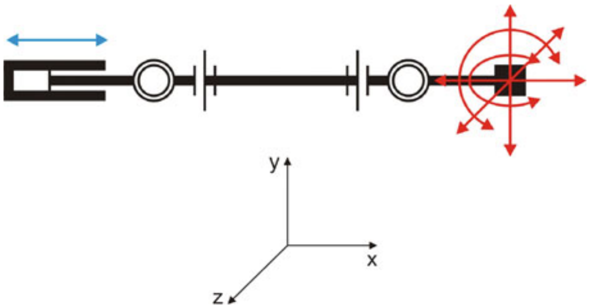

Fig. 7 $\underline{P}_zR_zR_zR_z$ limb

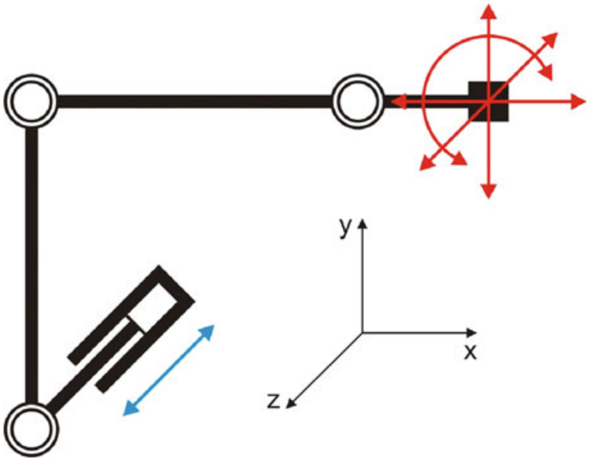

linear actuator ($\underline{P}$). An orthogonal parallel manipulator with three $\underline{P}$UU or $\underline{P}$RRRR limbs shows the following characteristics:

+ The maximum rotation angles of all the joints are similar.
– The installation size is large because of an in-line arrangement of the links and the linear actuator.

$\underline{P}$RRR limb (Fig. 7) has four degrees of freedom and comprises three parallel revolute joints (R) as well as one linear actuator ($\underline{P}$). An orthogonal parallel manipulator with three $\underline{P}$RRR limbs shows the following characteristics:

– The maximum rotation angle of the intermediate revolute joint is approximately two times larger than those of the peripheral revolute joints in case of the same link lengths in the limb.
+ Because of an angular arrangement of the links and the linear actuator, the installation size is small.

$\underline{\Pi}$RΠR limb (Fig. 8) has four degrees of freedom and comprises two parallel revolute joints (R) and two perpendicular parallelograms with four parallel revolute

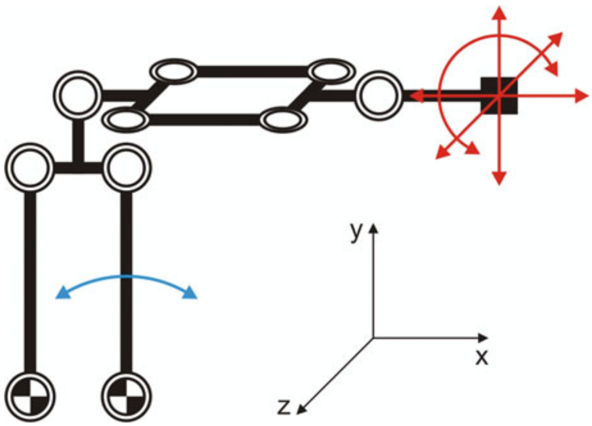

Fig. 8 $\underline{\Pi}_x R_z \Pi_z R_z$ limb

joints (Π). The parallelogram connected with the fixed base is driven ($\underline{\Pi}$). An orthogonal parallel manipulator with three $\underline{\Pi}$RΠR limbs shows the following characteristics:

+ The maximum rotation angles of all the joints are similar.
+ Because of an angular arrangement of the links, the installation size is small.

5 Monolithic Design

A micro manipulator to be monolithically designed is based on the implementation of the dimensioned right circular notch flexure hinge into the selected orthogonal parallel manipulator with three $\underline{\Pi}$RΠR limbs. A pseudo-rigid-body model (PRBM) [12] of the micro manipulator being composed of rigid links and conventional revolute joints instead of the flexure hinges is made. Using inverse kinematic calculation, the link lengths are so optimized that the maximum rotation angles of all the revolute joints are similar and not larger than ± 0.02 rad for the working space of the moving platform of 4 x 4 x 4 mm^3. The distances between the parallel revolute joints of 100 mm and 120 mm are assumed (Table 6).

A flexure hinge-based ΠRΠR limb is monolithically designed (Fig. 9). The limbs are firmly connected with a cubic moving platform (20 x 20 x 20 mm^3) in an orthogonal arrangement and orientation. The computer-aided design model of the micro manipulator is further analysed by means of finite-element method (FEM).

6 Results

The computer-aided design model is analysed with respect to the parasitic rotations of the moving platform (Table 7), the maximum stress in the flexure hinges (Table 8) and the stiffness of the micro manipulator (Table 9).

Displacing the moving platform to the border of the cubic working space (4 x 4 x 4 mm^3), parasitic rotations up to 0.4 mrad are obtained. A maximum stress

Table 6 Rotation angles of conventional revolute joints for given displacements of moving platform and optimized rigid link lengths in case of orthogonal parallel manipulator with ΠRΠR limbs (PRBM)

Displacements of moving platform [mm]			Rotation angles of joints [rad]											
			Joint 1			Joints 2, 3, 4, 5			Joint 6			Joints 7, 8, 9, 10		
			Limb X	Limb Y	Limb Z	Limb X	Limb Y	Limb Z	Limb X	Limb Y	Limb Z	Limb X	Limb Y	Limb Z
2	0	0	-0.0002	-0.0000	-0.0184	0.0000	**0.0202**	0.0000	0.0002	0.0000	0.0184	0.0168	0.0002	0.0032
2	2	0	-0.0186	-0.0002	-0.0184	-0.0000	**0.0202**	**0.0202**	0.0186	0.0002	0.0184	**0.0202**	0.0170	0.0034
2	2	2	-0.0186	-0.0186	-0.0186	**0.0202**	**0.0202**	**0.0202**	0.0186	0.0186	0.0186	**0.0202**	**0.0202**	**0.0202**

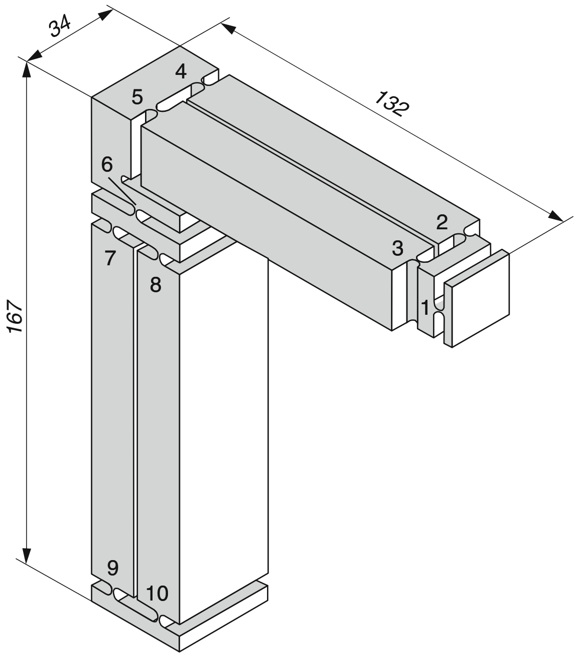

Fig. 9 Monolithic design of flexure hinge-based ΠRΠR limb (without drive unit)

Table 7 Displacements and corresponding parasitic rotations of moving platform (FEM)

	Case 1	Case 2	Case 3
x [mm]	2.0	2.0	2.0
y [mm]	0.0	2.0	2.0
z [mm]	0.0	0.0	2.0
θx [μrad]	1.4	-341.7	-212.4
θy [μrad]	129.3	130.7	-212.4
θz [μrad]	-343.0	-213.8	-212.4

Table 8 Maximum stress in flexure hinges (FEM)

	Case 1	Case 2	Case 3
Critical hinges	2,3,4,5	2,3,4,5	2,3,4,5
σ_{max} [MPa]	413.6	418.8	426.9

Table 9 Eigenmodes and eigenfrequencies of micro manipulator (FEM)

	Translation	Rotation
Non active drives	$\geq$ 19.7 Hz	$\geq$ 496.9 Hz
Active drives	-	$\geq$ 553.9 Hz

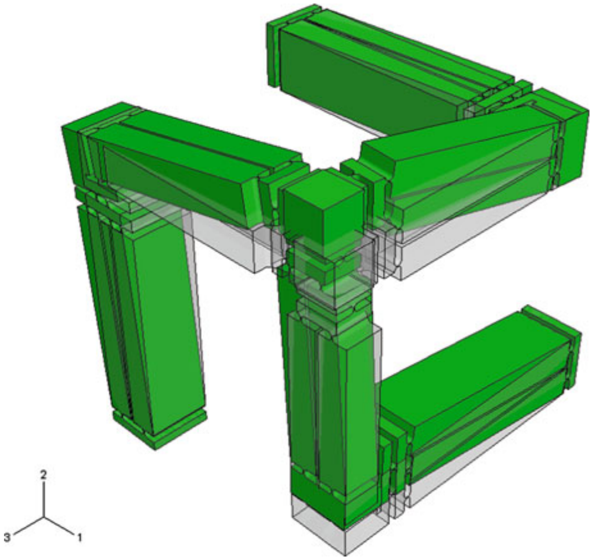

Fig. 10 First eigenmode when non active drives (19.7 Hz) (FEM)

in the flexure hinges up to 430 MPa is detected then. This stress value is in accordance with the calculation using equations (1)-(3) ($\sigma_{max} = 432.8$ MPa). As expected, the micro manipulator with non active drives (three translational degrees of freedom of the moving platform) possesses a low translation stiffness (20 Hz) (Fig. 10), but a high rotation stiffness (500 Hz). When the drives are active (no degrees of freedom of the moving platform), the rotation stiffness is even higher (550 Hz) (Fig. 11), while the translation stiffness is extremely high.

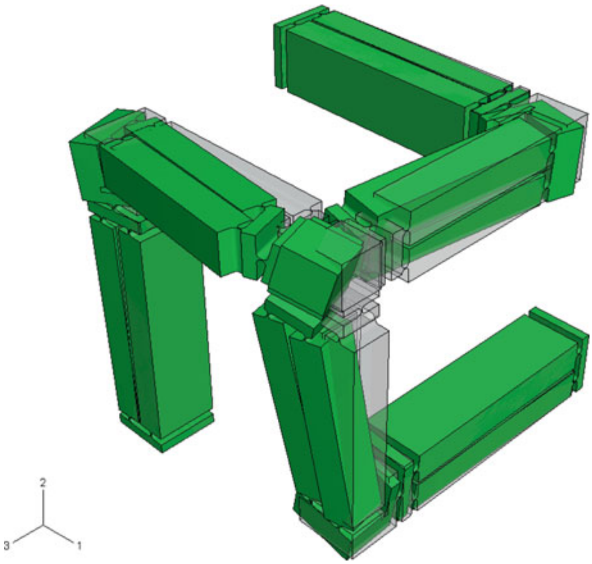

Fig. 11 First eigenmode when active drives (553.9 Hz) (FEM)

7 Summary

Two typical (corner filleted notch and right circular notch) flexure hinges are dimensioned according to the motion range and compared at first. The right circular notch flexure hinge shows more suitable characteristics (motion accuracy, torsion stiffness) for the implementation into a parallel manipulator. Using a systematic approach, three limb structures ($\underline{P}$RRRR, $\underline{P}$RRR and $\underline{\Pi}$RΠR) being able to build orthogonal parallel manipulators with a regular spatial translation of the moving platform are preselected and briefly assessed. Favourable characteristics of the $\underline{\Pi}$RΠR limb are highlighted. For the dimensioned right circular notch flexure hinge and the selected orthogonal parallel manipulator with three $\underline{\Pi}$RΠR limbs, a micro manipulator is monolithically designed and analysed. Thereby, small parasitic rotations of the moving platform and a high stiffness of the micro manipulators are achieved. Therefore, a further research through the realization and the test of an experimental model is intended.

References

1. Merlet, J.-P., Parallel robots, Springer, 2006.
2. Pernette, E., Henein, S., Magnani, I., Clavel, R., Design of parallel robots in microrobotics, Robotica, Vol. 15, 1997, 417-420.
3. Smith, S., T., Flexures, Elements of elastic mechanisms, Gordon and Breach, 2000.
4. Trease, B., P., Moon, Y.-M., Kota, S., Design of large-displacement compliant joints, Journal of mechanical design, Vol. 127, 2005, 788-798.
5. Lobontiu, N., Compliant mechanisms, Design of flexure hinges, CRC Press, 2003.
6. Xu, Q., Li, Y., Mechanical design of compliant parallel micromanipulators for nano scale manipulation, International conference on nano/micro engineered and molecular systems, 2006, 653-657.
7. Koseki, Y., Tanikawa, T., Koyachi, N., Arai, T., Kinematic analysis of translational 3-DoF micro parallel mechanism using matrix method, International conference on intelligent robots and systems, 2000, 786-792.
8. Koseki, Y., Arai, T., Sugimoto, K., Takatuji, T., Goto, M., Design and accuracy evaluation of high-speed and high precision parallel mechanism, International conference on robotics and automation, 1998, 1340-1345.
9. Herve, J., M., The Lie group of rigid body displacements, a fundamental tool for mechanism design, Mechanism and machine theory, Vol. 34, 1999, 719-730.
10. Kong, X., Gosselin, C., M., Type synthesis of 3-DoF translational parallel manipulators based on screw theory, Journal of mechanical design, Vol. 126, 2004, 83-92.
11. Carricato, M., Parenti-Castelli, V., A family of 3-DoF translational parallel manipulators, Journal of mechanical design, Vol. 125, 2003, 302-307.
12. Howell, L., L., Compliant mechanisms, Wiley, 2001